JHWCR JOURNAL OF HEALTH, WELLNESS AND COMMUNITY RESEARCH 3007-0570

https://doi.org/10.61919/m3y22007

Original Article

Comparative Analysis of Computed Tomography and Magnetic Resonance Imaging in the Evaluation of Congenital Thoracic Scoliosis

M Shahbaz[1], Ali Noman[2], Sehar Riaz[1], Sumaira Malik[1], Abeeyah Andleeb[1], Hafiz Sana Sarwar[1]

[1] Department of Medical Imaging Technology, Superior University, Lahore, Pakistan
[2] BSMIT, MS AHS(MIT), Superior University Lahore, Pakistan

*** Corresponding author: Sehar Riaz, seharriaz616@gmail.com**

ABSTRACT

Background: Congenital thoracic scoliosis is a structural spinal deformity caused by abnormal vertebral development and may be associated with occult neural axis abnormalities. Computed tomography provides detailed assessment of osseous malformations, whereas magnetic resonance imaging enables evaluation of the spinal cord and associated intraspinal abnormalities. **Objective:** To comparatively analyze CT and MRI findings in patients with congenital thoracic scoliosis and determine whether specific CT-detected vertebral anomalies are associated with MRI-detected neural axis abnormalities. **Methods:** A cross-sectional comparative imaging study was conducted at Ghurki Trust and Teaching Hospital, Lahore, over six months. Seventy-seven patients aged 11–19 years with congenital thoracic scoliosis who underwent both CT and MRI were included. CT findings included block vertebra, hemivertebra, vertebral anomalies, rib anomalies, and vertebral wedging/rotation, while MRI findings included tethered cord, diastematomyelia, and other neural axis abnormalities. Data were analyzed using SPSS version 25.0, with chi-square test, Fisher's exact test, t-test, ANOVA, odds ratios, and logistic regression applied where appropriate. **Results:** Tethered cord was detected in 19 patients (24.7%) and diastematomyelia in 24 patients (31.2%). Block vertebra showed a significant association with tethered cord ($\chi^2 = 5.229$, $p = 0.022$) and was an independent predictor of MRI-detected abnormality (adjusted OR = 5.344, 95% CI: 2.420–11.679; $p < 0.001$). Hemivertebra demonstrated a higher mean MRI anomaly burden than block vertebra in focused comparison (6.43 vs 4.39; $p = 0.002$), while overall differences across broader CT groups were not significant ($p = 0.126$). **Conclusion:** CT and MRI are complementary in evaluating congenital thoracic scoliosis. Block vertebra is a clinically important CT marker associated with MRI-detected tethered cord, supporting integrated imaging assessment for accurate diagnosis, neural risk detection, and preoperative planning. **Keywords:** Congenital thoracic scoliosis; computed tomography; magnetic resonance imaging; block vertebra; hemivertebra; tethered cord; diastematomyelia.

"Cite this Article" | Received: 10 March 2025; Accepted: 24 April 2026; Published: 06 May 2026.

Author Contributions: Concept: MS; Design: SR; Data Collection: SM and AA; Analysis: HSS; Supervision: AN; Drafting: MS. **Ethical Approval**: Superior University, Lahore, Pakistan. Informed Consent: Written informed consent was obtained from all participants; Conflict of Interest: The authors declare no conflict of interest; Funding: No external funding; Data Availability: Available from the corresponding author on reasonable request; Acknowledgments: N/A.

INTRODUCTION

Congenital thoracic scoliosis is a structural spinal deformity present from birth and results from abnormal vertebral development during embryogenesis. In this condition, defective formation or segmentation of the thoracic vertebrae produces a fixed lateral curvature of the spine, commonly accompanied by vertebral rotation and imbalance of the thoracic cage. Unlike postural or functional scoliosis, congenital thoracic scoliosis is caused by intrinsic osseous malformation, including hemivertebra, block vertebra, wedge vertebra, unilateral unsegmented bar, or mixed vertebral anomalies, each of which may influence curve progression differently during childhood and adolescence (1). The thoracic location is clinically important because spinal deformity in this region may alter rib

cage morphology, reduce pulmonary capacity, disturb cardiothoracic development, and contribute to functional limitation when progressive deformity is not detected and managed early (2).

The diagnostic evaluation of congenital thoracic scoliosis requires accurate characterization of both bony vertebral deformity and associated neural axis abnormalities. Computed tomography provides high-resolution visualization of osseous anatomy and is particularly useful for identifying hemivertebrae, fused vertebral segments, segmentation defects, abnormal pedicle morphology, vertebral rotation, rib anomalies, and complex three-dimensional spinal alignment (3). These features are essential for defining the anatomical basis of the deformity and for planning corrective procedures, especially when surgical treatment requires precise assessment of vertebral morphology and spatial relationships (4). However, although CT is highly informative for bone detail, its use in pediatric and adolescent populations must be balanced against radiation exposure, making it important to identify the clinical contexts in which CT findings add meaningful diagnostic or management value (5).

Magnetic resonance imaging complements CT by providing superior assessment of the spinal cord, conus medullaris, nerve roots, intervertebral discs, and surrounding soft tissues without ionizing radiation. In patients with congenital scoliosis, MRI is particularly important because neural axis abnormalities such as tethered cord, syringomyelia, diastematomyelia, Chiari malformation, split cord malformation, and intraspinal lipoma may remain clinically silent but substantially influence surgical risk, neurological outcome, and timing of intervention (6). MRI therefore has a central role in identifying occult intraspinal pathology before deformity correction, while CT remains valuable for defining the osseous architecture responsible for the spinal curvature (7). The two modalities should not be viewed as interchangeable; rather, they provide complementary information, with CT defining the structural skeletal abnormality and MRI determining whether clinically significant neural involvement is present (8).

Previous literature supports the need for integrated imaging assessment in congenital spinal deformity. Morphological studies have shown that hemivertebra characteristics, location, and asymmetry are associated with scoliosis severity and progression, emphasizing the prognostic relevance of detailed vertebral evaluation (9). Contemporary reviews of congenital scoliosis further highlight the complex interaction between genetic, embryologic, skeletal, and neurological factors, supporting the need for multidisciplinary diagnostic strategies and individualized management (10). Evidence also suggests that bony vertebral malformations are frequently accompanied by spinal cord anomalies, and that the likelihood of neural axis pathology may increase with the complexity and number of congenital vertebral defects (11). Despite this, uncertainty remains regarding which specific CT-detected vertebral anomalies most strongly correspond to MRI-detected neural axis abnormalities in patients with congenital thoracic scoliosis.

This uncertainty creates an important clinical and research gap. In routine practice, patients with congenital thoracic scoliosis may undergo both CT and MRI, yet the predictive relationship between CT-defined vertebral abnormalities and MRI-defined neural axis findings is not always clearly established. Better understanding of this relationship may help clinicians identify patients who require more urgent or comprehensive MRI evaluation, refine preoperative risk assessment, reduce missed occult neural pathology, and support safer treatment planning. In PICO terms, the population of interest is patients with congenital thoracic scoliosis; the index findings are CT-detected vertebral anomalies such as block vertebra, hemivertebra, and other structural malformations; the comparative or correlative modality is MRI; and the clinically relevant outcomes are neural axis abnormalities including tethered cord and diastematomyelia. Therefore, this study aimed to comparatively analyze CT and MRI findings in congenital thoracic scoliosis and to determine whether specific CT-detected vertebral anomalies are associated with MRI-detected neural axis abnormalities, with the hypothesis that selected structural vertebral defects are linked to a higher burden of occult intraspinal pathology (12).

MATERIALS AND METHODS

A cross-sectional comparative imaging study was conducted at Ghurki Trust and Teaching Hospital, Lahore, over a six-month period after approval of the research synopsis. The study was designed to evaluate the complementary diagnostic role of computed tomography and magnetic resonance imaging in patients with congenital thoracic scoliosis by comparing CT-detected vertebral abnormalities with MRI-detected neural axis abnormalities. Eligible participants were patients aged 11 to 19 years who had clinical or imaging features suggestive of congenital thoracic scoliosis and who underwent both CT and MRI examinations as part of their diagnostic evaluation. Participants were selected using a convenience sampling technique from patients presenting to the clinical setting during the study period. Written informed consent was obtained from each participant or from a parent or guardian where required, and only those who fulfilled the predefined eligibility criteria were included.

Patients were included if they had congenital thoracic scoliosis, were within the specified age range, had undergone both CT and MRI examinations of diagnostic quality, and were willing to participate. Patients were excluded if they had a history of prior corrective or decompressive spinal surgery, idiopathic scoliosis, neuromuscular scoliosis, degenerative scoliosis, trauma-related scoliosis, incomplete imaging with only CT or only MRI, poor-quality imaging due to motion or technical artefacts, unsafe radiation exposure conditions, or severe cardiopulmonary comorbidities limiting imaging feasibility. These criteria were applied to ensure that the study population represented congenital thoracic scoliosis cases in which direct comparison between CT-based osseous findings and MRI-based neural axis findings could be performed reliably.

The estimated sample size was calculated using the single-proportion formula, $n = Z^2P(1 - P)/d^2$, with a 95% confidence level, an assumed prevalence proportion of 0.05, and a 5% margin of error, yielding a final sample size of 77 participants. Each participant underwent CT and MRI evaluation according to standardized institutional imaging procedures. CT imaging was performed using a 16-slice Toshiba computed tomography scanner with the patient in the supine position. Thin-slice helical acquisition was obtained across the thoracic spine, with multiplanar reconstruction and three-dimensional reconstruction used to evaluate vertebral morphology, segmentation defects, hemivertebra, block vertebra, vertebral rotation, pedicle morphology, rib anomalies, and other osseous abnormalities. Pediatric dose-reduction principles were applied where appropriate to minimize radiation exposure while maintaining diagnostic image quality.

MRI was performed using 0.4 Tesla and 1.5 Tesla Canon magnetic resonance imaging systems with the patient in the supine position. Imaging covered the spine sufficiently to assess spinal curvature, spinal cord morphology, conus position, intraspinal pathology, and associated neural axis abnormalities. Standard sagittal and axial T1-weighted and T2-weighted sequences were obtained, with STIR sequences used where clinically appropriate to assess cord signal abnormality, edema, syrinx formation, and soft-tissue changes. MRI variables included the presence or absence of tethered cord, diastematomyelia, syringomyelia, Chiari malformation, split cord malformation, intraspinal lipoma, and other clinically relevant neural axis abnormalities. CT and MRI findings were recorded using a structured data collection form that also included demographic characteristics, clinical history, presenting symptoms, and relevant imaging observations.

The primary imaging variables were CT-detected vertebral anomalies and MRI-detected spinal or neural axis abnormalities. CT findings were operationally categorized as block vertebra, hemivertebra, vertebral anomaly, rib anomaly, vertebral wedging, or other structural abnormalities according to radiological appearance. MRI findings were categorized according to the presence or absence of tethered cord, diastematomyelia, syringomyelia, and other intraspinal anomalies. The main outcome of interest was the association between specific CT findings and MRI-detected abnormalities. Additional outcomes included the distribution of CT and MRI findings, the frequency of combined abnormalities, the strength

of association between selected CT and MRI variables, and the mean burden of MRI abnormalities across CT-defined groups.

To reduce information bias, imaging findings were recorded systematically using predefined variables. CT and MRI findings were interpreted from diagnostic-quality images, and cases with severe artefacts or incomplete imaging were excluded. Selection bias was addressed by applying uniform inclusion and exclusion criteria to all eligible participants during the study period. Confounding was considered by documenting demographic and clinical variables and by applying multivariable analysis where appropriate to assess whether selected CT findings independently predicted MRI abnormalities. Data consistency was maintained through structured recording of all variables, coding of categorical responses, and review of entered data before analysis.

Data were analyzed using IBM SPSS version 25.0 and Microsoft Excel 2016. Descriptive statistics were used to summarize demographic and imaging characteristics. Frequencies and percentages were calculated for categorical variables, including sex distribution, CT findings, and MRI abnormalities. Means and standard deviations were calculated for continuous or count-based variables, including the number of MRI abnormalities across CT-defined groups. Associations between categorical CT and MRI findings were assessed using chi-square tests or Fisher's exact tests where cell counts required exact testing. Odds ratios with 95% confidence intervals were calculated to quantify the strength of association between selected CT findings and MRI abnormalities. Independent-samples t-tests were used to compare mean MRI abnormality burden between two CT-defined groups, while one-way analysis of variance was used to compare mean MRI abnormality burden across more than two CT categories. Levene's test was applied to assess homogeneity of variance before group mean comparisons. Multivariable logistic regression was used to assess the independent influence of CT findings on MRI-detected spinal abnormalities, with regression coefficients, p-values, adjusted odds ratios, and 95% confidence intervals reported where applicable. A p-value of less than 0.05 was considered statistically significant.

Missing or incomplete records were handled by excluding cases with unavailable paired CT and MRI data or non-diagnostic image quality from comparative analysis. Data were entered in coded form to preserve confidentiality, and all patient identifiers were removed from the analytical dataset. Ethical principles were followed throughout the study, including informed consent, confidentiality of patient data, voluntary participation, and minimization of imaging-related risk. CT imaging was limited to clinically justified examinations, and MRI was used as a radiation-free modality for evaluating neural axis abnormalities. The final dataset was stored securely, and access was restricted to authorized research personnel to maintain data integrity, reproducibility, and participant privacy.

RESULTS

A total of 77 patients with congenital thoracic scoliosis underwent both CT and MRI evaluation. The cohort included 43 females (55.8%) and 34 males (44.2%). CT findings included block vertebra, hemivertebra, vertebral anomalies, rib anomalies, and vertebral wedging/rotation, while MRI findings included tethered cord and diastematomyelia as the main neural axis abnormalities analyzed.

Table 1. Baseline Demographic and Key Imaging Characteristics of the Study Population

Variable	Category	Frequency (n)	Percentage (%)
Gender	Female	43	55.8
Gender	Male	34	44.2
Total sample	—	77	100.0
Block vertebra on CT	Yes	68	88.3
Block vertebra on CT	No	9	11.7

Variable	Category	Frequency (n)	Percentage (%)
Hemivertebra on CT	Yes	71	92.2
Hemivertebra on CT	No	6	7.8
Vertebral anomalies on CT	Yes	70	90.9
Vertebral anomalies on CT	No	7	9.1
Tethered cord on MRI	Yes	19	24.7
Tethered cord on MRI	No	58	75.3
Diastematomyelia on MRI	Yes	24	31.2
Diastematomyelia on MRI	No	53	68.8

The study population showed a slight female predominance, with females representing 55.8% of the sample. CT-detected vertebral abnormalities were common, particularly hemivertebra, observed in 71 of 77 patients (92.2%), followed by vertebral anomalies in 70 patients (90.9%) and block vertebra in 68 patients (88.3%). MRI identified tethered cord in 19 patients (24.7%) and diastematomyelia in 24 patients (31.2%), indicating that approximately one-quarter to one-third of the cohort had clinically relevant neural axis abnormalities.

Table 2. Association Between CT-Detected Block Vertebra and MRI-Detected Tethered Cord

Block Vertebra on CT	Tethered Cord: Yes, n (%)	Tethered Cord: No, n (%)	Total	Test Statistic	p-value
Yes	14 (20.6)	54 (79.4)	68	$\chi^2 = 5.229$	0.022
No	5 (55.6)	4 (44.4)	9	Fisher's exact test	0.036
Total	19 (24.7)	58 (75.3)	77	—	—

A statistically significant association was found between block vertebra on CT and tethered cord on MRI. Among patients with block vertebra, 14 of 68 (20.6%) had tethered cord, while 54 of 68 (79.4%) did not. Among patients without block vertebra, 5 of 9 (55.6%) had tethered cord and 4 of 9 (44.4%) did not. The Pearson chi-square test showed statistical significance ($\chi^2 = 5.229$, $p = 0.022$), and Fisher's exact test was also significant ($p = 0.036$), demonstrating a non-random distribution of tethered cord across block vertebra groups.

Table 3. Associations Between Selected CT Findings and MRI-Detected Neural Axis Abnormalities

CT Finding	MRI Finding	CT Finding Present: MRI Yes / No	CT Finding Absent: MRI Yes / No	Total Cases	Statistical Test	p-value
Vertebral anomalies	Diastematomyelia	21 / 49	3 / 4	77	Pearson $\chi^2 = 0.490$	0.484
Vertebral anomalies	Diastematomyelia	21 / 49	3 / 4	77	Fisher's exact test	0.671
Hemivertebra	Tethered cord	16 / 55	3 / 3	77	Pearson $\chi^2 = 2.245$	0.134
Hemivertebra	Tethered cord	16 / 55	3 / 3	77	Fisher's exact test	0.156

Vertebral anomalies were present in 70 patients, of whom 21 (30.0%) had diastematomyelia and 49 (70.0%) did not. Among the 7 patients without vertebral anomalies, 3 (42.9%) had diastematomyelia and

4 (57.1%) did not. The association between vertebral anomalies and diastematomyelia was not statistically significant ($\chi^2 = 0.490$, $p = 0.484$; Fisher's exact $p = 0.671$). Hemivertebra was present in 71 patients, of whom 16 (22.5%) had tethered cord and 55 (77.5%) did not. Among the 6 patients without hemivertebra, 3 (50.0%) had tethered cord and 3 (50.0%) did not. The association between hemivertebra and tethered cord was also not statistically significant ($\chi^2 = 2.245$, $p = 0.134$; Fisher's exact $p = 0.156$).

Table 4. Comparison of MRI Anomaly Burden Across CT-Defined Groups

CT Finding Group	n	Mean MRI Anomalies	SD	SE	95% CI for Mean	Minimum	Maximum	Inferential Test	p-value
Block vertebra	26	4.30	2.10	0.33	3.65–4.95	1.00	8.00	One-way ANOVA, F = 2.12	0.126
Hemivertebra	33	5.10	2.50	0.39	4.70–5.50	2.00	9.00	One-way ANOVA, F = 2.12	0.126
Other CT findings	18	3.80	1.90	0.30	3.40–4.20	2.00	7.00	One-way ANOVA, F = 2.12	0.126
Total	77	4.07	2.19	0.20	3.67–4.47	1.00	9.00	Levene's test, F = 0.679	0.507

The mean number of MRI anomalies was highest in the hemivertebra group (5.10 ± 2.50), followed by the block vertebra group (4.30 ± 2.10) and the other CT findings group (3.80 ± 1.90). Although the numerical pattern showed a higher MRI anomaly burden among patients with hemivertebra, the overall group difference was not statistically significant on one-way ANOVA ($F = 2.12$, $p = 0.126$). Homogeneity of variance was supported by Levene's test based on mean values ($F = 0.679$, $p = 0.507$).

A focused two-group comparison showed a significant difference between the block vertebra and hemivertebra groups. Patients in the hemivertebra group had a higher mean number of MRI anomalies (6.43 ± 1.434) than those in the block vertebra group (4.39 ± 2.173). The mean difference was −2.040, with a 95% confidence interval from −3.268 to −0.811, and the difference was statistically significant ($t = -3.398$, $p = 0.002$).

Table 5. Multivariable Logistic Regression Assessing CT Findings and MRI-Detected Abnormalities

Variable	B Coefficient	Wald	p-value	Adjusted OR, Exp(B)	95% CI Lower	95% CI Upper
Intercept	1.245	6.021	0.014	3.467	1.215	9.616
CT: Block vertebra	1.678	13.676	<0.001	5.344	2.420	11.679
CT: Hemivertebra	−0.432	4.337	0.037	0.649	0.430	0.984
MRI anomaly: Yes	2.101	7.539	0.006	8.189	2.112	31.921
Treatment group	0.562	3.100	0.078	1.756	0.923	3.337

In the multivariable model, block vertebra was a statistically significant predictor, with an adjusted odds ratio of 5.344 and a 95% confidence interval of 2.420–11.679 ($p < 0.001$). Hemivertebra showed a negative coefficient ($B = -0.432$) and an adjusted odds ratio of 0.649 with a 95% confidence interval of 0.430–0.984 ($p = 0.037$). MRI anomaly status showed the largest odds ratio in the model (OR = 8.189, 95% CI:

2.112–31.921, p = 0.006). The treatment group variable showed a non-significant trend (OR = 1.756, 95% CI: 0.923–3.337, p = 0.078).

Overall, the results demonstrated that CT and MRI findings were complementary in the evaluation of congenital thoracic scoliosis. Block vertebra showed a statistically significant association with tethered cord in categorical analysis, while hemivertebra showed a higher mean MRI anomaly burden in focused group comparison. Across the broader CT-defined categories, however, the mean MRI anomaly burden did not differ significantly, indicating that MRI-detected neural axis abnormalities were not uniformly distributed according to CT category alone.

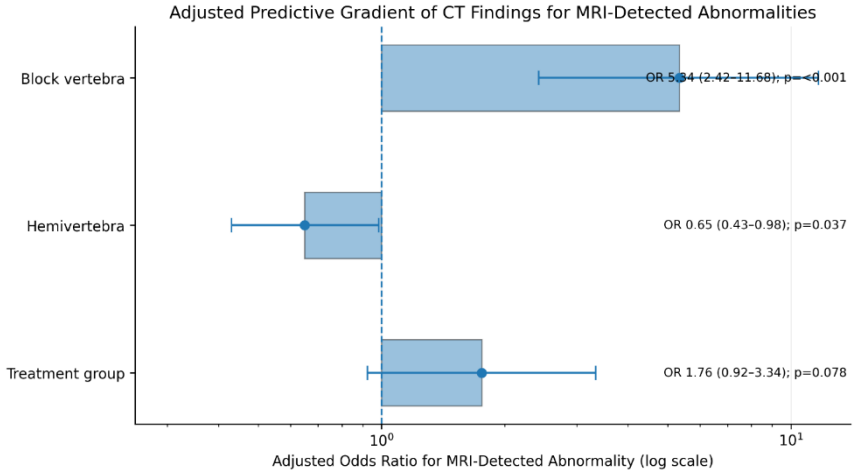

Figure 1. Adjusted Predictive Gradient of CT Findings for MRI-Detected Abnormalities

The figure demonstrates a clear adjusted risk gradient across CT-defined predictors of MRI-detected abnormalities. Block vertebra showed the strongest independent association, increasing the odds of MRI-detected abnormality more than fivefold (adjusted OR = 5.34, 95% CI: 2.42–11.68; p < 0.001). Hemivertebra showed an inverse adjusted association (adjusted OR = 0.65, 95% CI: 0.43–0.98; p = 0.037), while the treatment group variable showed a non-significant positive trend (adjusted OR = 1.76, 95% CI: 0.92–3.34; p = 0.078). The confidence interval for block vertebra remained entirely above the null value, supporting its clinical relevance as the most prominent CT-based predictor of MRI-detected neural axis abnormality in this cohort.

DISCUSSION

This cross-sectional comparative imaging study demonstrates that CT and MRI provide complementary information in the evaluation of congenital thoracic scoliosis, with CT defining the structural vertebral deformity and MRI identifying clinically important neural axis abnormalities. In this cohort of 77 patients, CT-detected vertebral abnormalities were frequent, particularly hemivertebra, vertebral anomalies, and block vertebra, while MRI detected tethered cord in 24.7% and diastematomyelia in 31.2% of patients. These findings support the concept that congenital thoracic scoliosis should not be assessed only as a bony spinal deformity, because a meaningful proportion of patients also demonstrate associated intraspinal abnormalities that may influence neurological risk, operative planning, and long-term management (13).

The strongest categorical association was observed between CT-detected block vertebra and MRI-detected tethered cord. Block vertebra showed a statistically significant relationship with tethered cord, indicating that segmentation-related vertebral fusion may be linked with abnormal neural axis development or altered cord biomechanics. Embryologically, vertebral segmentation and spinal cord development occur through closely related developmental processes, and disruption during early formation may produce combined osseous and neural abnormalities. Clinically, this association is important because tethered cord may remain occult until neurological deterioration, pain, weakness,

bladder dysfunction, or postoperative complications occur. Therefore, identification of block vertebra on CT should raise the level of suspicion for associated neural axis pathology and supports the value of MRI in patients with congenital thoracic scoliosis who show complex segmentation defects (14).

Hemivertebra was common in the study population and showed a higher mean burden of MRI abnormalities compared with block vertebra in the focused two-group comparison. This finding suggests that asymmetric vertebral formation defects may be associated with a greater overall load of MRI-detectable abnormalities, possibly because hemivertebra can generate asymmetric growth, vertebral rotation, and progressive curvature during skeletal development. However, the categorical association between hemivertebra and tethered cord was not statistically significant, which indicates that hemivertebra may contribute more to the overall burden or severity pattern of MRI abnormalities rather than acting as a single direct predictor of tethered cord. This distinction is clinically relevant because it shows that the interpretation of CT findings should not rely only on one binary association, but should consider the total deformity pattern and the possibility of multiple coexisting neural abnormalities (15).

The relationship between vertebral anomalies and diastematomyelia was not statistically significant despite a larger absolute number of diastematomyelia cases among patients with vertebral anomalies. This result suggests that broad CT categories such as “vertebral anomalies” may be too heterogeneous to predict a specific MRI abnormality reliably. Diastematomyelia and other split cord malformations may arise from complex embryologic mechanisms involving notochordal, mesenchymal, and neural tube development rather than from a single identifiable bony defect. Therefore, the absence of a statistically significant association does not exclude clinical relevance, but it does indicate that generalized vertebral anomaly labels should be interpreted cautiously when estimating the likelihood of split cord malformation (16).

The multivariable analysis further emphasized the predictive importance of selected CT findings. Block vertebra showed the strongest adjusted association with MRI-detected abnormality, with an adjusted odds ratio greater than five. This indicates that block vertebra may represent a higher-risk structural marker within the congenital scoliosis spectrum. In contrast, hemivertebra showed an inverse adjusted association in the model, despite showing a higher mean MRI anomaly burden in the focused comparison. This apparent difference may reflect overlap among CT categories, subgroup imbalance, small cell counts, or differences between categorical prediction and mean anomaly burden analysis. Such findings highlight the complexity of congenital spinal deformity data, where individual patients may have more than one vertebral abnormality and where the same CT label may not carry identical clinical meaning across all patients (17).

The overall ANOVA comparison did not show a statistically significant difference in mean MRI anomaly burden across block vertebra, hemivertebra, and other CT finding groups. This finding suggests that although selected pairwise comparisons may identify important differences, CT classification alone may not fully explain the distribution of MRI-detected abnormalities. Congenital thoracic scoliosis is often a mixed developmental condition rather than a single isolated vertebral defect, and neural axis abnormalities may be influenced by the number, type, level, and complexity of vertebral malformations. This supports a combined imaging approach rather than reliance on CT alone to decide whether neural axis evaluation is necessary (18).

The findings have practical implications for imaging pathways in congenital thoracic scoliosis. CT remains highly valuable for identifying vertebral architecture, pedicle morphology, rib anomalies, segmentation defects, hemivertebra, block vertebra, and three-dimensional deformity, particularly when surgical planning is being considered. MRI, however, is essential for detecting tethered cord, diastematomyelia, syringomyelia, split cord malformation, and other occult neural abnormalities that may not be visible on CT. The current results reinforce that CT and MRI answer different but interdependent clinical questions: CT defines the skeletal deformity, while MRI determines whether the spinal cord and neural structures are involved. In patients with block vertebra, hemivertebra, or complex

vertebral malformation patterns, MRI adds clinically meaningful information that may alter management decisions (19).

These results should also be interpreted in light of the study design. The use of convenience sampling and a single-center setting may limit generalizability. Some CT categories appear to overlap, which is expected in congenital scoliosis but can complicate statistical interpretation if analyses are not clearly separated into patient-level and finding-level comparisons. The relatively small number of patients without certain CT findings may reduce statistical power for subgroup comparisons and may widen confidence intervals. In addition, congenital scoliosis is influenced by curve severity, vertebral level, number of anomalous segments, associated rib anomalies, and neurological symptoms, and these factors may affect the likelihood of MRI abnormalities. Despite these limitations, the study provides useful evidence that specific CT findings, particularly block vertebra, may help identify patients at increased risk of MRI-detected neural axis abnormalities.

Overall, the study supports the complementary use of CT and MRI in congenital thoracic scoliosis. The statistically significant association between block vertebra and tethered cord, together with the increased MRI anomaly burden observed in selected CT-defined groups, indicates that structural vertebral malformations may serve as important markers for underlying neural axis pathology. The absence of significant associations for some CT–MRI comparisons further emphasizes that no single CT finding can completely rule in or rule out neural involvement. A comprehensive imaging strategy that integrates CT-based skeletal assessment with MRI-based neural evaluation remains essential for accurate diagnosis, safe treatment planning, and improved clinical decision-making in patients with congenital thoracic scoliosis.

CONCLUSION

This study concludes that CT and MRI play complementary roles in the evaluation of congenital thoracic scoliosis, with CT providing detailed assessment of vertebral and rib abnormalities and MRI identifying associated neural axis abnormalities that may not be clinically apparent. Among the CT findings, block vertebra showed the strongest association with MRI-detected tethered cord and emerged as an important imaging marker for possible underlying neural involvement. Hemivertebra was associated with a higher mean burden of MRI abnormalities in focused comparison, suggesting that asymmetric vertebral formation defects may contribute to more complex spinal and neural imaging patterns. However, not all CT-detected vertebral anomalies showed statistically significant associations with specific MRI abnormalities, indicating that CT findings alone are insufficient to exclude occult intraspinal pathology. These findings support the integrated use of CT and MRI in patients with congenital thoracic scoliosis, particularly when block vertebra, hemivertebra, or complex vertebral malformations are present, to improve diagnostic accuracy, guide preoperative planning, reduce neurological risk, and support individualized clinical management.

REFERENCES

1. Cheng JC, Castelein RM, Chu WCW, Danielsson AJ, Dobbs MB, Grivas TB, et al. Adolescent idiopathic scoliosis. Nat Rev Dis Primers. 2015;1:15030.

2. Kwon JW, Son S, Lee J, Lee G, Kang H, Oh J, et al. Incidence rate of congenital scoliosis estimated from a nationwide health insurance database. Sci Rep. 2021;11:5507.

3. Liu Y, Zhuang Q, Li L, Wang B, Zhang J, Zhou Y. Asymmetric biomechanical characteristics of the paravertebral muscle in adolescent idiopathic scoliosis. Clin Biomech. 2019;65:81–6.

4. Chang DG, Suk SI, Kim JH, Ha KY, Na KH, Lee JH. Surgical outcomes by age at the time of surgery in the treatment of congenital scoliosis in children under age 10 years. Spine J. 2015;15:1783–95.

5. Hedequist D, Emans J. Congenital scoliosis. J Am Acad Orthop Surg. 2004;12(4):266–75.

6. Arlet V, Odent T, Aebi M. Congenital scoliosis. Eur Spine J. 2003;12(5):456–63.

7. Hedequist D, Emans J. Congenital scoliosis. J Pediatr Orthop. 2007;27(1):106–16.

8. Elsebai HB, Yazici M, Thompson GH, Emans JB, Skaggs DL, Crawford AH, et al. Safety and efficacy of growing rod technique for pediatric congenital spinal deformities. J Pediatr Orthop. 2011;31(1):1–5.

9. Mohanty SP, Pai Kanhangad M, Narayana Kurup JK, Saiffudeen S. Vertebral, intraspinal and other organ anomalies in congenital scoliosis. Eur Spine J. 2020;29(10):2449–56.

10. Furdock R, Brouillet K, Luhmann SJ. Organ system anomalies associated with congenital scoliosis: a retrospective study of 305 patients. J Pediatr Orthop. 2019;39(3):e190–4.

11. Farley FA, Loder RT, Nolan BT, Dillon MT, Frankenburg EP, Kaciroti NA, et al. Mouse model for thoracic congenital scoliosis. J Pediatr Orthop. 2001;21(4):537–40.

12. Giampietro PF, Blank RD, Raggio CL, Merchant S, Jacobsen FS, Faciszewski T, et al. Congenital and idiopathic scoliosis: clinical and genetic aspects. Clin Med Res. 2003;1(2):125–36.

13. Maisenbacher MK, Han JS, O'Brien ML, Tracy MR, Erol B, Schaffer AA, et al. Molecular analysis of congenital scoliosis: a candidate gene approach. Hum Genet. 2005;116(5):416–9.

14. Wu N, Ming X, Xiao J, Wu Z, Chen X, Shinawi M, et al. TBX6 null variants and a common hypomorphic allele in congenital scoliosis. N Engl J Med. 2015;372(4):341–50.

15. Kawakami N, Tsuji T, Yanagida H, Uno K, Matsumoto M, Watanabe K, et al. Radiographic analysis of the progression of congenital scoliosis with rib anomalies during the growth period. ArgoSpine News J. 2012;24(1–2):56–61.

16. Tauchi R, Tsuji T, Cahill PJ, Flynn JM, Glotzbecker M, et al. Reliability analysis of Cobb angle measurements of congenital scoliosis using X-ray and 3D-CT images. Eur J Orthop Surg Traumatol. 2016;26(1):53–7.

17. Nagayoshi R, Kawakami N, Misayaka K. Morphological analysis of intervertebral disc by magnetic resonance imaging in patients with congenital scoliosis exhibiting formation failure. J Spine Res. 2011;2:1745–9.

18. Gao Z, Wang Z, Liu J, Niu B, Yang W, Wang Y, et al. Evaluation of renal function in children with congenital scoliosis and congenital anomalies of the kidney and urinary tract. Med Sci Monit. 2018;24:4667–78.

19. Demirkiran HG, Bekmez S, Celilov R, Ayvaz M, Dede O, Yazici M. Serial derotational casting in congenital scoliosis as a time-buying strategy. J Pediatr Orthop. 2015;35(1):439.